Available online at www.sciencedirect.com
ScienceDirect
International Journal of Heat and Fluid Flow 28 (2007) 262–267
International Journal of HEAT AND FLUID FLOW
www.elsevier.com/locate/ijhff

Flow and heat transfer over a rotating disk with surface roughness

Myung Sup Yoon [a], Jae Min Hyun [a,*], Jun Sang Park [b]

[a] Department of Mechanical Engineering, Korea Advanced Institute of Science and Technology, 373-1 Kusong-dong, Yusong-gu, Taejon 305-701, South Korea
[b] Department of Mechanical Engineering, Halla University, San 66, HeungUp, Wonju, Kangwon-do 220-712, South Korea

Received 10 May 2005; received in revised form 10 January 2006; accepted 13 April 2006
Available online 28 July 2006

Abstract

A numerical study is made of flow and heat transfer near an infinite disk, which rotates steadily about the longitudinal axis. The surface of the disk is characterized by axisymmetric, sinusoidally-shaped roughness. The representative Reynolds number is large. Numerical solutions are acquired to the governing boundary-layer-type equations. The present numerical results reproduce the previous data for a flat disk. For a wavy surface disk, the radial distributions of local skin friction coefficient and local Nusselt number show double periodicity, which is in accord with the previous results. Physical explanations are provided for this finding. The surface-integrated torque coefficient and average Nusselt number increase as the surface roughness parameter increases. The effect of the Rossby number is also demonstrated.
© 2006 Elsevier Inc. All rights reserved.

Keywords: Rotating disk flow; Wavy disk; Sinusoidal disk; Boundary layer flow; Torque coefficient; Rossby number

1. Introduction

Flow of an incompressible viscous fluid over a steadily-rotating disk constitutes a long-standing subject. The classical model of von Karman (1921) dealt with an infinite disk, which rotates at a rotation rate Ω^*, and the fluid far away from the disk is assumed to be at rest. The mathematical development utilized the similarity variable approach, and numerical solutions to the resulting ordinary differential equations were acquired. The solution delineated the salient qualitative characteristics of the flow, and this model has since occupied the center stage. The determination of three-component velocity field and the calculation of the torque exerted on the disk have been the major issues. The ensuing investigations, e.g., Cochran, 1934, Rogers and Lance, 1960, Benton, 1966, extended the problem by introducing modified solution procedures. Recently, these rotating disk problems find industrial applications, e.g., liquid film phenomena in wafer processing (Rahman and Faghri, 1992; Yevtushenko and Chapovska, 1996; Ozar et al., 2004), shrouded rotating disk modeling in gas turbine engines (Phadke and Owen, 1988; Long, 1994), rotating disk reactor (RDR) in chemical vapor deposition (CVD) processes (Evans and Greif, 1987; Winters et al., 1997).

In the majority of prior studies, the disk surface is assumed to be flat and smooth. From the standpoint of practical engineering applications, the effect of the roughness of the disk surface on the global flow field and the resulting friction coefficient warrants an in-depth scrutiny. The present paper intends to provide descriptions of flow in the vicinity of a rotating disk with rough surface.

For a definitive problem formulation, the profile of rough surface is modeled by sinusoids which are axisymmetric with respect to the axis of rotation, as was done by Le Palec et al. (1990). The transformed boundary-layer equations are derived, which subsequently are solved numerically. For technological applications, the torque coefficient and the heat transfer coefficient, as the amplitude and wavelength of the surface roughness vary, are of particular interest.

2. Formulation and numerical procedures

A disk of infinite radius rotates steadily about the central axis at a rotation rate Ω^* in an incompressible viscous

* Corresponding author. Tel.: +82 42 869 3012; fax: +82 42 869 3210.
E-mail address: jmhyun@kaist.ac.kr (J.M. Hyun).

0142-727X/$ - see front matter © 2006 Elsevier Inc. All rights reserved.
doi:10.1016/j.ijheatfluidflow.2006.04.008

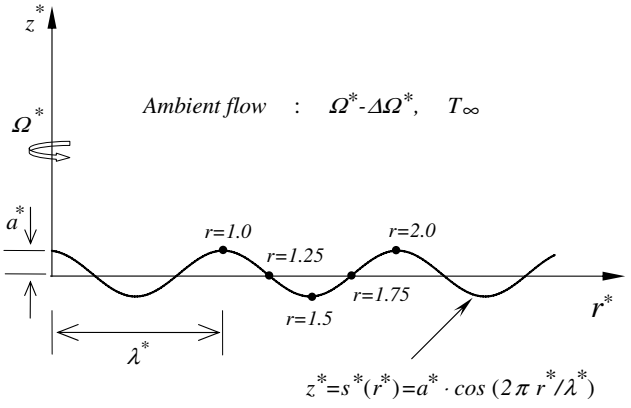

Fig. 1. Flow geometry.

fluid. The properties of the fluid are density (ρ), coefficient of viscosity (μ), kinematic viscosity (ν), thermal conductivity (K_f), and specific heat at constant pressure (C_p). The ambient fluid far away from the disk rotates at rotation rate $\Omega_f^*[\equiv \Omega^* - \Delta\Omega^*]$, and the temperature is T_∞. The Rossby number of the system is defined $Ro \equiv \Delta\Omega^*/\Omega^*$, and, in the present paper, $0 \leqslant Ro \leqslant 1$.

A cylindrical frame (r^*, θ^*, z^*), rotating together with the far-field ambient fluid at Ω_f^*, is adopted. The velocity components in this coordinate system are denoted by (u^*, v^*, w^*). The geometrical layout is sketched in Fig. 1. The surface of the disk $s^*(r^*)$ is described as

$$z^* = s^*(r^*) = a^* \cdot \cos(2\pi r^*/\lambda^*), \tag{1}$$

in which a^* is the amplitude and λ^* the wavelength of the wavy surface. In the present study, as guided by Le Palec et al. (1990), the heat flux (q) at the disk surface is assumed to be constant, i.e., $q = \text{const}$.

The nondimensionalized governing axisymmetric Navier–Stokes equations, in the rotating frame, are (Greenspan, 1968)

$$\frac{1}{r}\frac{\partial(ru)}{\partial r} + \frac{\partial w}{\partial z} = 0, \tag{2}$$

$$Ro\left(u\frac{\partial u}{\partial r} - \frac{v^2}{r} + w\frac{\partial u}{\partial z}\right) = -\frac{\partial p}{\partial r} + 2(1-Ro)v + E\left[\frac{1}{r}\frac{\partial}{\partial r}\left(r\frac{\partial u}{\partial r}\right) + \frac{\partial^2 u}{\partial z^2} - \frac{u}{r^2}\right], \tag{3}$$

$$Ro\left(u\frac{\partial v}{\partial r} + \frac{uv}{r} + w\frac{\partial v}{\partial z}\right) = -2(1-Ro)u + E\left[\frac{1}{r}\frac{\partial}{\partial r}\left(r\frac{\partial v}{\partial r}\right) + \frac{\partial^2 v}{\partial z^2} - \frac{v}{r^2}\right], \tag{4}$$

$$Ro\left(u\frac{\partial w}{\partial r} + w\frac{\partial w}{\partial z}\right) = -\frac{\partial p}{\partial z} + E\left[\frac{1}{r}\frac{\partial}{\partial r}\left(r\frac{\partial w}{\partial r}\right) + \frac{\partial^2 w}{\partial z^2}\right], \tag{5}$$

$$Ro\left(u\frac{\partial \theta}{\partial r} + w\frac{\partial \theta}{\partial z}\right) = \frac{E}{Pr}\left[\frac{1}{r}\frac{\partial}{\partial r}\left(r\frac{\partial \theta}{\partial r}\right) + \frac{\partial^2 \theta}{\partial z^2}\right], \tag{6}$$

The boundary conditions are expressed as

$$\left.\begin{aligned} u = w = 0, \quad v = r, \\ \frac{\partial\theta}{\partial n} = -\lambda^*\left(\frac{\Omega^*}{\nu}\right)^{1/2} \end{aligned}\right\} \quad \text{at} \quad z = \delta\cdot\cos(2\pi r), \tag{7}$$

$$u = v = \theta = 0 \quad \text{as} \quad z \to \infty. \tag{8}$$

In the above, the nondimensional variables are defined as

$$(u, v, w) = \frac{(u^*, v^*, w^*)}{Ro\cdot\Omega^*\lambda^*},$$

$$(r, z) = \frac{1}{\lambda^*}(r^*, z^*),$$

$$p = \frac{p^*}{Ro\cdot\rho\Omega^{*2}\lambda^{*2}},$$

$$\theta = \frac{(T - T_\infty)}{q}\left(\frac{\Omega^*}{\nu}\right)^{1/2} K_f,$$

$$\delta = \frac{a^*}{\lambda^*}.$$

It is advantageous to transform the wavy surface into a flat surface in the $[\xi - \eta]$ domain by using the transformation of Prandtl (Yao, 1988),

$$\begin{aligned} \xi &= r, \\ \eta &= z - s(r), \end{aligned} \tag{9}$$

where $s(r) = \delta\cdot\cos(2\pi r)$. In the $[\xi - \eta]$ coordinates, the velocity components (U,W) are expressed as

$$\begin{bmatrix} U \\ W \end{bmatrix} = J\cdot\begin{bmatrix} \xi_r & \xi_z \\ \eta_r & \eta_z \end{bmatrix}\begin{bmatrix} u \\ w \end{bmatrix} = \begin{bmatrix} u \\ -s'u + w \end{bmatrix},$$

in which J is the Jacobian of transformation. It is worth noting that the s' and s'' indicate, respectively, the first and second differentiations of s with respect to r, i.e., $s' = ds^*/dr^* = ds/dr$ and $s'' = ds'/dr$.

In the present investigation, rapidly-rotating fluid systems are of interest, i.e., $E \ll 1$, which are relevant to many technological applications. Thus, attention is focused on the boundary-layer type flows close to the disk surface. For a thin boundary layer, the variables are re-scaled:

$$\begin{aligned} \zeta &= E^{-1/2}\eta, \\ \tilde{w} &= E^{-1/2}W. \end{aligned} \tag{10}$$

By substituting ζ and $\tilde{w}$ into the transformed governing equations, and neglecting the higher-order terms, the boundary-layer equations are obtained:

$$u/r + u_r + \tilde{w}_\zeta = 0 \tag{11}$$

$$Ro\cdot(uu_r + \tilde{w}u_\zeta) = -p_r + E^{-1/2}s'p_\zeta + (1+s'^2)u_{\zeta\zeta} + v(2(1-Ro) + Ro\cdot v/r) \tag{12}$$

$$Ro\cdot s''u^2 = s'p_r - E^{-1/2}(1+s'^2)p_\zeta - s'v(2(1-Ro) + Ro\cdot v/r) \tag{13}$$

$$Ro\cdot(uv_r + \tilde{w}v_\zeta) = (1+s'^2)v_{\zeta\zeta} - u(2(1-Ro) + Ro\cdot v/r) \tag{14}$$

$$Ro\cdot(u\theta_r + \tilde{w}\theta_\zeta) = \frac{(1+s'^2)}{Pr}\theta_{\zeta\zeta} \tag{15}$$

In the above, $E \equiv Re^{-1}$ is the Ekman number based on the wavelength of the roughness λ^*, $Re \equiv \Omega^* \lambda^{*2}/\nu$.

In line with the analysis of von Karman (1921) for an infinite disk, the pressure gradient in the radial direction is taken to be zero, i.e.,

$$p_r = 0. \tag{16}$$

The above assumption, which was invoked by Le Palec et al. (1990), is justified when the surface roughness is mild, i.e., when the amplitude/wavelength ratio δ is small.

Combining Eqs. (12), (13) and (16) produces

$$Ro \cdot (u u_r + \tilde{w} u_\zeta) = -\frac{s' s''}{1+s'^2} Ro \cdot u^2 + (1+s'^2) u_{\zeta\zeta} + \frac{1}{1+s'^2} v(2(1-Ro) + Ro \cdot v/r). \tag{17}$$

Introducing the variables

$$f = \frac{u}{r} = \frac{F}{Ro}, \quad g = \frac{v}{r} = \frac{G}{Ro}, \quad h = \tilde{w} = \frac{H}{Ro} \tag{18}$$

the equations are re-written as

$$2f + r\frac{\partial f}{\partial r} + \frac{\partial h}{\partial \zeta} = 0, \tag{19}$$

$$Ro\left(rf\frac{\partial f}{\partial r} + h\frac{\partial f}{\partial \zeta} + f^2\left(1 + r\frac{s' s''}{1+s'^2}\right)\right) = (1+s'^2)\frac{\partial^2 f}{\partial \zeta^2} + \frac{g}{1+s'^2}(2(1-Ro) + Ro \cdot g), \tag{20}$$

$$Ro\left(rf\frac{\partial g}{\partial r} + h\frac{\partial g}{\partial \zeta} + fg\right) = (1+s'^2)\frac{\partial^2 g}{\partial \zeta^2} - f(2(1-Ro) + Ro \cdot g), \tag{21}$$

$$Ro\left(rf\frac{\partial \theta}{\partial r} + h\frac{\partial \theta}{\partial \zeta}\right) = \frac{(1+s'^2)}{Pr}\frac{\partial^2 \theta}{\partial \zeta^2} \tag{22}$$

$$f = h = 0, \quad g = 1, \quad \frac{\partial \theta}{\partial \zeta} = -\frac{1}{(1+s'^2)^{1/2}} \quad \text{at} \quad \zeta = 0 \tag{23}$$

$$f = g = 0, \quad \theta = 0 \quad \text{as} \quad \zeta \to \infty. \tag{24}$$

Obviously, for a flat disk rotating in a quiescent fluid, $Ro = 1$, and the above equations are reduced to the familiar ordinary differential equations of von Karman (see, e.g., Schilichting, 1979), i.e.,

$$H' = -2F, \quad F'' = -G^2 + F^2 + F'H, \quad G'' = 2FG + HG'. \tag{25}$$

Numerical solutions to the array of partial differential Eqs. (19)–(22) were acquired. The numerical procedures were based on the finite difference method. The derivatives with respect to r were discretized by backward differencing, and central differencing was utilized for the ζ-derivatives. At every r-station, computations were iterated until the relative errors of two successive iterations became less than 10^{-4} (Yao, 1983; Cheng and Wang, 2000). After several trials, the ζ-grid interval was set at 0.1, and the r-grid interval at 0.02. The differences between the results for grid of $\Delta\zeta = 0.1$, $\Delta r = 0.02$ and those for grid of $\Delta\zeta = 0.05$, $\Delta r = 0.01$ were less than 2% in the local Nu and the skin friction coefficient for $Pr = 0.7$, $\delta = 0.1$. A large number of validation tests were performed for the previously-studied problems (Rogers and Lance, 1960; Yao, 1983; Le Palec et al., 1990). The numerical results were highly consistent with the published data.

With the numerically-computed flow details in hand, the local skin-friction coefficient C_f and the torque coefficient C_M are the important quantities in engineering analyses. The local shear stress τ_w in the azimuthal direction is computed as

$$\tau_w = \mu \left.\frac{\partial v^*}{\partial n^*}\right|_{z^* = s^*(r^*)} = Ro\mu\Omega^* \left.\frac{\partial v}{\partial n}\right|_{z = s(r)} = Ro\mu\Omega^*(1+s'^2)^{1/2} Re^{1/2} \left.\frac{\partial v}{\partial \zeta}\right|_{\zeta = 0}, \tag{26}$$

and C_f is defined as

$$C_f \equiv \frac{-2\tau_w}{\rho r^{*2}\Omega^{*2}} = -2Ro(1+s'^2)^{1/2} Re_{r^*}^{-1/2} \left.\frac{\partial g}{\partial \zeta}\right|_{\zeta = 0}. \tag{27}$$

It follows that the total torque $\overline{T}$, up to a finite radial position $r^* = R^*$, is calculated as:

$$\overline{T} = \int_S r^* \tau_w \mathrm{d}S = \int_0^{R^*} 2\pi r^{*2} \tau_w (1+s'^2)^{1/2} \mathrm{d}r^*, \tag{28}$$

and the torque coefficient C_M is

$$C_M \equiv \frac{-4\overline{T}}{\rho R^{*5}\Omega^{*2}} = -8\pi Ro Re_{R^*}^{-1/2} \int_0^{R^*} r^{*3}(1+s'^2) \left.\frac{\partial g}{\partial \zeta}\right|_{\zeta = 0} / R^{*4} \mathrm{d}r^*. \tag{29}$$

In the above, Re_{R*} denotes the Reynolds number based on the finite radius R^*, and Re_{r*} is the Reynolds number based on the local position r^* (see, Takhar et al., 2002).

In a similar manner, the local Nusselt number is defined:

$$Nu = \frac{h_c \lambda^*}{K_f}, \tag{30}$$

where h_c is the local heat transfer coefficient. From the condition of constant wall heat flux q,

$$h_c = \frac{q}{T_w - T_\infty}, \tag{31}$$

where T_w denotes the wall temperature. It then follows from Eqs. (30) and (31) that:

$$Nu Re^{-1/2} = \frac{1}{\theta_w}. \tag{32}$$

Also, as in Le Palec et al. (1990), the average Nusselt number for a rough surface, $\overline{Nu}$, and that for a flat disk, $\overline{Nu}_p$, are derived:

$$\overline{Nu}Re^{-1/2} = \frac{1}{S}\int_S NuRe^{-1/2}\mathrm{d}S, \tag{33}$$

$$\overline{Nu}_\mathrm{p} = \overline{Nu}\frac{S}{\pi R^{*2}}, \tag{34}$$

where S is the surface area of the wavy disk.

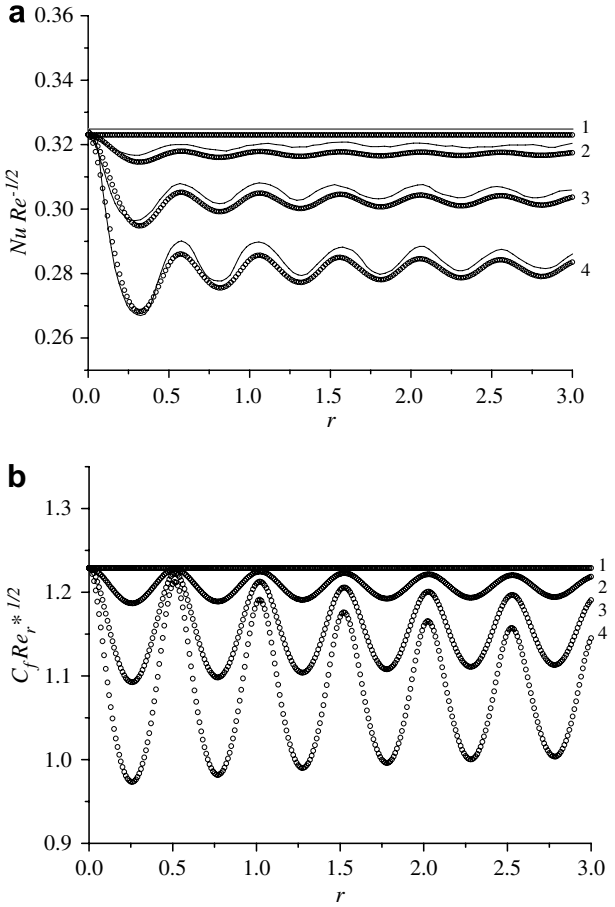

Fig. 2. The local Nusselt number ($NuRe^{-1/2}$) and the local skin friction coefficient ($C_\mathrm{f}Re_{r*}^{1/2}$) variations. $Ro = 1.0$. $Pr = 0.7$. —, Le Palec et al. (1990); °, the present results. Curves are for: (1) $\delta = 0$; (2) $\delta = 1/16$; (3) $\delta = 1/8$; (4) $\delta = 1/5$.

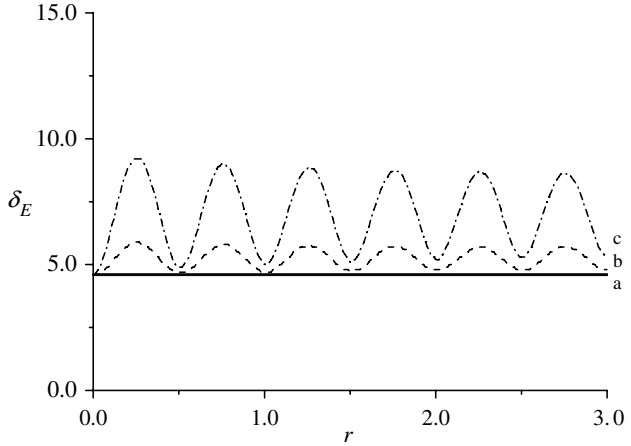

Fig. 3. Ekman boundary layer thickness (δ_E) variations. $Ro = 1.0$. Curves are for: (a) $\delta = 0$; (b) $\delta = 1/10$; (c) $\delta = 1/5$.

3. Results and discussion

In a similar problem setting, for a special case of $Ro = 1.0$, Le Palec et al. (1990) presented the numerically-obtained data for Nu. As illustrated in Fig. 2(a), the data of Le Palec et al. (1990) are in close agreement with

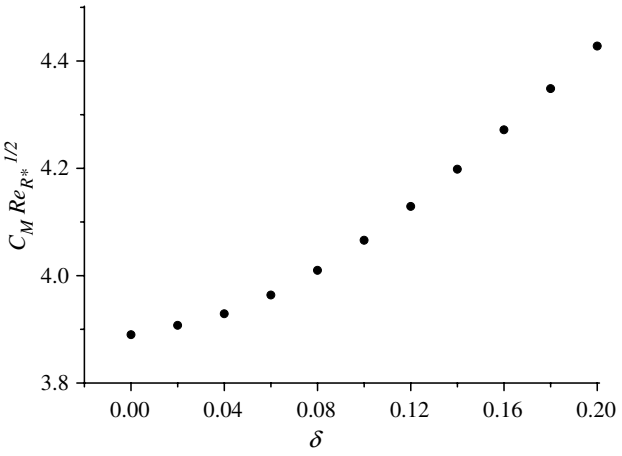

Fig. 4. Torque coefficient ($C_\mathrm{M}Re_{R*}^{1/2}$) vs. δ. $N = 3.0$, $Ro = 1.0$.

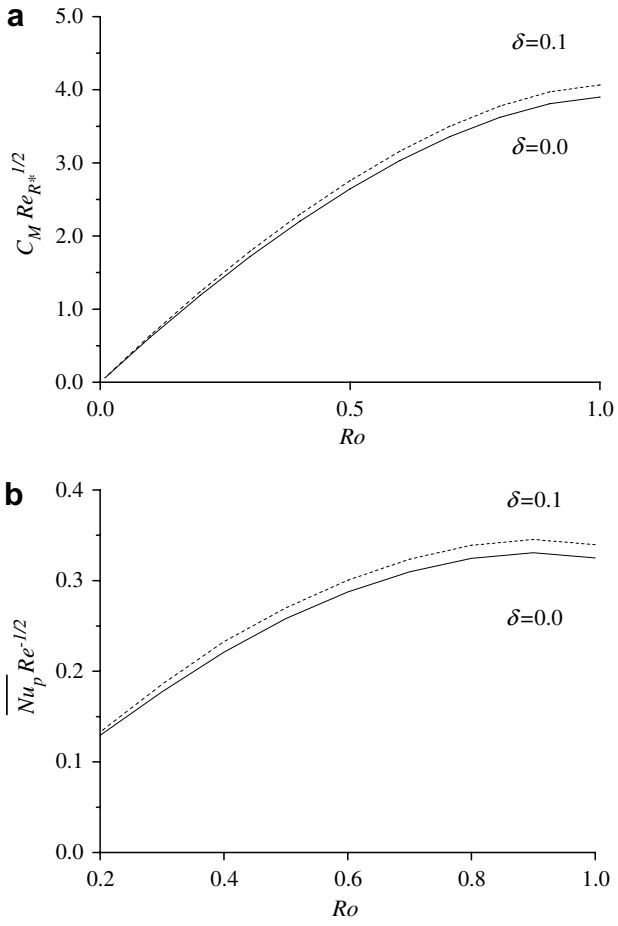

Fig. 5. Rossby number (Ro) effect on (a) C_M; (b) $\overline{Nu}_\mathrm{p}$.

the present results. It is noted that the study of Le Palec et al. (1990) was restricted to the case of $Ro = 1.0$, i.e., the far-field ambient fluid was at rest. Furthermore, descriptions of the flow field were not presented in Le Palec et al. (1990). It is evident in Fig. 2(a) that the spatial variations of Nu undergo two cycles over a wavelength of surface profile, i.e., the wavelength of $Nu(r)$ is $\lambda^*/2$ in dimensional terms.

Fig. 2(b) illustrates the behavior of C_f, which shows the radial variation over the wavelength $\lambda^*/2$. The local skin friction coefficient (C_f) is computed as in Eq. (27). This is similar to the behavior of Nu. The value of C_f for a flat disk is well-known, $C_f Re_{r*}^{1/2} = 1.23$ (see $G'(0)$ at Rogers and Lance, 1960). In general, in the presence of the surface roughness, C_f is smaller than for a flat disk, which implies that the local shear stress is reduced due to the boundary-layer thickening.

This observation can also be explained by using the following argument. Since the surface area is slanted to the vertical, the effective rotation rate for the localized surface area under consideration is $\Omega^* \cdot \cos\beta$, where β is the angle between $\vec{n}$ and $\vec{z}$. Therefore, the effective local Ekman layer is gauged by E_β $[\equiv \frac{\nu}{\Omega^* \cos\beta \lambda^{*2}}]$. Clearly, E_β depends only on the magnitude of β, not the sign, since $\cos(-\beta) = \cos\beta$. Therefore, the general pattern of flow variation is characterized by two cycles over the radial distance of one wavelength of surface variation. Fig. 3 displays the variations of the Ekman boundary layer thickness, δ_E, in the r direction. Here, δ_E defined as the height where $v^* = 0.02 r^* \Omega^*$. It is discernible that the boundary layer is thicker near the nodes than near the trough and crest. Therefore, the local minima of Nu and C_f appear at the node, and the local maxima of Nu and C_f are found at the trough and crest. The global maximum values of Nu and C_f are seen at the axis where the thickness of boundary layer is minimal.

The torque coefficient (C_M), defined in Eq. (29), is plotted in Fig. 4. Expectedly, as the amplitude a^* of the surface roughness increases, the increase in C_M is appreciable. It is remarked that C_M is calculated as a surface integral of shear stress; therefore, the effect of area increment is incorporated in the computation of C_M.

It is now of interest to explore the effect of the Rossby number, Ro. Fig. 5 illustrates that, as Ro increases, both the skin friction and associated heat transfer increase, as anticipated. For a lager value of Ro, the difference in rotation rates between the disk and the ambient flow increases, which strengthens the boundary layer near the disk surface. The detailed profiles of the radial and azimuthal velocity components are exhibited in Fig. 6. The results for a flat ($\delta = 0$) and wavy disks ($\delta \neq 0$) are displayed. It is also shown here that the flat-disk results are in close agreement with the previous data of Rogers and Lance (1960).

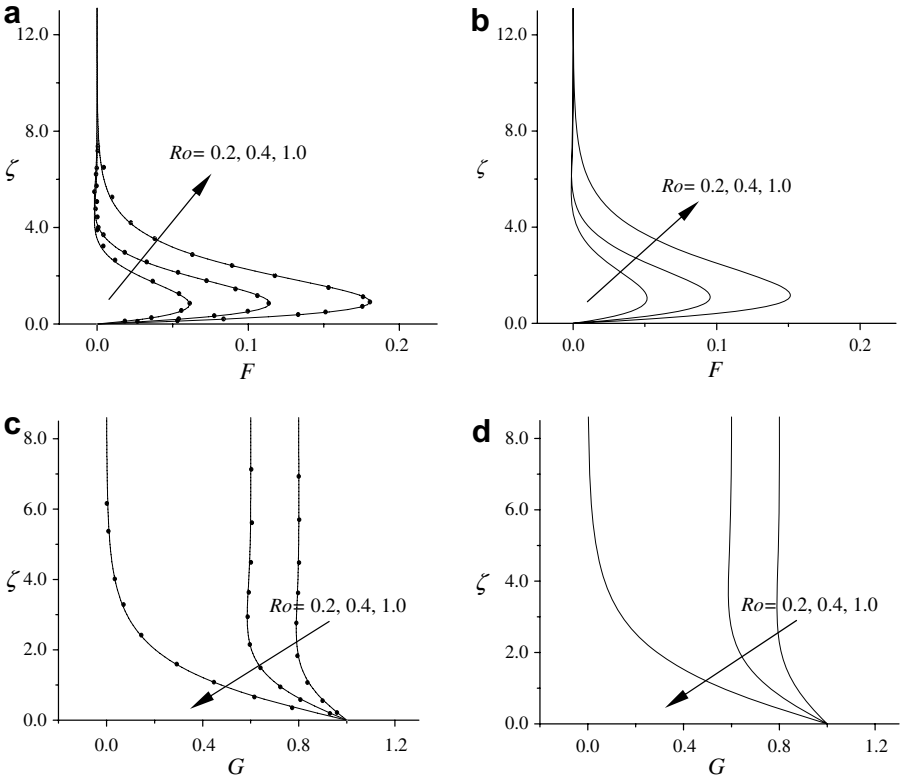

Fig. 6. Rossby number (Ro) effect on the velocity profile. Dots are results from Rogers and Lance, 1960. (a) Radial velocity profile (F) for a flat disk. (b) Radial velocity profile (F) for a wavy disk ($\delta = 0.1$, $r = 1.75$). (c) Azimuthal velocity profile (G) for a flat disk. (d) Azimuthal velocity profile (G) for a wavy disk ($\delta = 0.1$, $r = 1.75$).

4. Conclusion

Rotating flow induced by an infinite sinusoidal wavy disk is studied. Using Prandtl's transformation (1988), boundary layer type equations are acquired. Numerical results show broad agreement with theoretical and experimental work by Le Palec et al. (1990). However, no detailed flow information was provided in Palec. In the present study, descriptions are given of the effect of surface roughness on C_f and C_M. The local quantities, such as Nu and C_f, show double periodicity. Physical explanations are offered by inspecting the variations of δ_E at the node, crest and trough position of a wavy disk. For a disk with surface roughness, the values of Nu and C_f are lower than those for a flat disk. As δ increases, the rise in C_M is appreciable. As Ro decreases, both $\overline{Nu}_p$ and C_M are reduced. The present numerical results demonstrate the structures of radial and azimuthal velocity profiles as Ro varies.

References

Benton, E.R., 1966. On the flow due to a rotating disk. J. Fluid Mech. 24, 781–800.

Cheng, C.Y., Wang, C.C., 2000. Forced convection in micropolar fluid flow over a wavy surface. Numer. Heat Transfer A 37, 271–287.

Cochran, W.G., 1934. The flow due to a rotating disk. Proc. Cambridge Philos. Soc. 30, 365–375.

Evans, G., Greif, R., 1987. A numerical model of the flow and heat transfer in a rotating disk chemical vapor deposition reactor. ASME J. Heat Transfer 109, 928–935.

Greenspan, H.P., 1968. The Theory of Rotating Fluids. Cambridge University Press, Cambridge.

Le Palec, G., Nardin, P., Rondot, D., 1990. Study of laminar heat transfer over a sinusoidal shaped rotating disk. Int. J. Heat Mass Transfer 33, 1183–1192.

Long, C.A., 1994. Disk heat transfer in a rotating cavity with an axial throughflow of cooling air. Int. J. Heat Fluid Flow 15, 307–316.

Ozar, B., Cetegen, B.M., Faghri, A., 2004. Experiments on heat transfer in a thin liquid film flowing over a rotating disk. ASME J. Heat Transfer 126, 184–192.

Phadke, U.P., Owen, J.M., 1988. Aerodynamic aspects of the sealing of gas-turbine rotor-stator systems. Part 1: the behavior of simple shrouded rotating-disk systems in a quiescent environment. Int. J. Heat Fluid Flow 9, 98–105.

Rahman, M.M., Faghri, A., 1992. Analysis of heating and evaporation from a liquid film adjacent to a horizontal rotating disk. Int. J. Heat Mass Transfer 35, 2655–2664.

Rogers, M.H., Lance, G.N., 1960. The rotationally symmetric flow of a viscous fluid in the presence of an infinite rotating disk. J. Fluid Mech. 7, 617–631.

Schilichting, H., 1979. Boundary layer theory. McGraw-Hill, New York.

Takhar, H.S., Singh, A.K., Nath, G., 2002. Unsteady mhd flow and heat transfer on a rotating disk in an ambient fluid. Int. J. Therm. Sci. 41, 147–155.

von Karman, T., 1921. Uber laminare und turbulente Reibung. Z. Agnew. Math. Mech. 1, 233–252.

Winters, W.S., Evans, G.H., Greif, R., 1997. Mixed binary convection in a rotating disk chemical vapor deposition reactor. Int. J. Heat Mass Transfer 40, 737–744.

Yao, L.S., 1983. Natural convection along a vertical wavy surface. ASME J. Heat Transfer 105, 465–468.

Yao, L.S., 1988. A note on Prandtl's transposition theorem. ASME J. Heat Transfer 110, 507–508.

Yevtushenko, A., Chapovska, R., 1996. Effect of a thin film on the heat distribution between a stationary pin and a rotating disk. Numer. Heat Transfer A 30, 835–848.